RC23872 (W0602-085) February 9, 2006
Electrical Engineering

IBM Research Report

Prediction of Losses Caused by Roughness of Metallization in Printed-Circuit Boards

A. Deutsch, C. W. Surovic, R. S. Krabbenhoft[1],
G. V. Kopcsay, B. J. Chamberlin[2]
IBM Research Division
Thomas J. Watson Research Center
P.O. Box 218
Yorktown Heights, NY 10598

[1]IBM Server Group
Rochester, MN 55901

[2]IBM Microelectronics Division
Endicott, NY 13760

Research Division
Almaden - Austin - Beijing - Haifa - India - T. J. Watson - Tokyo - Zurich

Prediction of Losses Caused by Roughness of Metallization in Printed-Circuit Boards

A. Deutsch, C. W. Surovic, R. S. Krabbenhoft[1], G. V. Kopcsay, B. J. Chamberlin[2]
IBM T. J. Watson Research Center, 1101 Kitchawan Road, Yorktown heights, NY 10598
Phone: (914) 945-2858, Fax: (914) 945-2141, email: deutsch@us.ibm.com
[1]IBM Server Group, Rochester, MN 55901
[2]IBM Microelectronics Division, Endicott, NY 13760

Abstract – In this paper the effect of metal roughness on the total loss, the extracted tanδ, and signal integrity of typical interconnections found in printed-circuit boards is extracted from measurements on three different materials. The differing characteristics of the roughened metal cross sections is highlighted, and a simplified, practical, two-dimensional, causal, broadband modeling methodology is shown.
Keywords: Printed circuit board losses, metallization roughness, characterization of card wiring permittivity.

Introduction

It has been shown by many researchers that the increase in the data-rates propagated on interconnections used on printed-circuit boards requires more accurate and causal transmission-line models for predicting system performance. The random data-patterns encountered on long signal paths have very fast risetimes commensurate with data-rates of 2-10 Gbps, in the order of 30-200 ps. At the same time, the long spans of steady-state levels caused by adjacent 0's or 1's require broadband causal models over the range DC to about 50 GHz. Such models need to accurately account for resistive and dielectric losses. Non-causal models can cause inaccurate signal integrity and timing prediction and circuit simulator convergence problems. Printed-circuit board fabricators are hard at work developing lower loss insulator materials to make the high data-rates possible. Such new material characterization needs to be made on multi-layer representative card structures. Oftentimes, dielectric constant and dielectric loss are obtained at a few frequencies, using several, non-consistent techniques and based on bulk material builds. Such techniques might also miss inhomogeneities in the effective dielectric properties that are of interest for signal propagation on typical card wiring. It will be shown that roughness of metallization needed to promote adhesion could add significant resistive losses, especially at high frequencies. The new materials could have higher moisture absorption properties that could increase loss and affect reliability. The new requirements for lead-free compatibility impose manufacturing constraints that could affect the electrical characteristics. It is important to accurately separate the resistive and dielectric losses for these new materials and to extract the material characteristics over the entire frequency range of interest. Single value dielectric constant $\varepsilon_r^{'}$ and dielectric loss $\tan\delta$ supplied by vendors today cannot be used to generate broadband causal models [1-2]. In addition, when used in system performance evaluations, erroneous predictions would occur as shown in Figs. 1 and 2. Three cases are compared, namely, with the use of broadband complex permittivity ε(ω), with constant $\varepsilon_r^{'}$ and no dielectric loss, and with constant $\varepsilon_r^{'}$ and constant tanδ. Even though the total attenuation in Fig. 1 with single value $\varepsilon_r^{'}$ and tanδ agrees fairly well at a target 3 GHz frequency with the broadband model, when used in actual simulations in Fig. 2, for a 3 Gbps signal and 76 cm long line, it is found that the actual propagated signals are quite different. Fig. 3 shows another example of representative stripline structures that were modeled with only skin-effect (tanδ = 0), with skin-effect and roughness (tanδ = 0), and with skin-effect, rough ridges, and complex frequency-dependent permittivity. The increase in attenuation due to dielectric loss starts to substantially dominate resistive losses for the lower resistance, 5-mil wide lines, even at as low a frequency as 5 GHz. Roughness also contributes a substantial amount to total loss. It should be noted that when roughness is accounted for separately, without being attributed to tanδ, the start of dominance of tanδ over skin effect is shifted to a higher frequency. Thus for 3 mil line, it starts at > 10 GHz instead of 4.6 GHz, for 4 mil lines starts at 10 GHz instead of 3 GHz, and for 5 mil lines at 4.6 GHz instead of 2.5 GHz.

In this study, three different insulator materials were used to build the same card design. In each case, two cards were fabricated, with and without roughened metallization, and the total loss was extracted over the range 10 KHz to 50 GHz. This paper will show how significant the loss due to roughness is, how it affects the accuracy of the model generation, the signal integrity, the board fabrication development, and the difficulty in modeling this effect.

Test Vehicle Configurations

The same design was used for all the three different printed-circuit board materials used, namely A, B, and C. A single stripline with additional top and bottom pad layers form a total thickness of under 635 μm (25 mil). 100-μm (4.0 mil) wide, 32-μm (1.26 mil) thick single lines are attached to very small surface pads through 203-μm (8-mil) diameter vias. The design is optimized to reduce the discontinuities introduced by pads, vias, and probes at the ends of the signal lines. The build for the card materials C and B were duplicated with and without roughened copper metallization. Card A was built with the standard process and with a very low profile roughening. Some typical profiles are shown in Fig. 4 for signal and ground plane layers for materials A, B, and C. The important part to notice is the difference in rough ridge profile between signal layer and ground layer, and between cards. Each card was made by a different manufacturer. Material A profile is shown in Fig. 5.

Notice the ridges on the side of the signal lines in addition to the top and the very high irregularity on the ground plane for card A in Fig. 4. Fig. 6 shows a very close view of the ridge tips. It can be seen that micro-nodules are electroplated that could be in size from 0.1 to 1 μm to promote adhesion. This increases surface area without adding to the overall topography. In addition, the side of the ridges and the conductor outline could have a thin layer of an organo-metallic compound. This will differ depending on whether the manufacturer used standard, reverse, or dual treatment. It is explained in [5-6] that standard treatment would be applied to the toothed, or non-drum side of the copper foil and was generally used on the three cards shown here. Fig. 6 shows a typical view of this alloy layer. The metals that are used can have resistivity that is more than an order of magnitude higher than for copper.

Eight cross sections were taken at various positions along the lines and one parallel to the length of the lines. It was found that for the card A, the low profile, LP, case, had the ridge height in the range of 2.5-5 μm, and for the rough case, 7.5-10 μm. For card B, the rough signal layer had ridges that were on the average 7.5 μm tall and 8 μm wide. The ground layer had 5.5 μm heights and 7.4 μm widths. For card C, the signal layer had heights of 5.3 μm and widths of 10.3 μm and for the ground layer, heights of 7.5 μm and widths of 8.6 μm. For typical copper resitivity of 2 μΩcm, skin-depth is in the range of 1.03 to 0.36 μm for 5 GHz to 40 GHz. This means, that the dimension of the ridges are larger than the skin-depth and the current will follow the contour of the ridges and increase the effective resistance and inductance and slow-down the wave propagation. The higher resistivity coating on the surface of the ridges will exacerbate this effect. Moreover, the irregularity of the random ridges could generate some non-TEM components of the field longitudinally and further affect the wave propagation.

DC Analysis

The resistance, capacitance, and cross sectional dimensions were analyzed for all six cards in order to ensure that similar conditions were used for comparison and the data is shown in the table below. Given the fact that these parts came from three different manufacturers, it is believed that the results were quite close. Resistivity was obtained from cross sectional dimensions and four-point resistance measurements. Line capacitance and dielectric constants $\varepsilon_r^{'}$ were obtained at 1 MHz. $\varepsilon_r^{'}$ was obtained from measuring the capacitance of a 12.7-mm (500-mil) diameter circular plate placed on the signal layer. It is observed that the effective DC resistivity increased only in the range of 0.05 – 0.6%. The effective dielectric constant increased by 2.4-4.3% at 1 MHz. Card B had the largest area difference between smooth and rough cards, namely 8.6%. The other two had very similar dimensions with ΔArea = 1.9-4.8%. The resultant line capacitance changed by only 1.2-3.1% due to roughness. If the cross section is slightly smaller and the dielectric constant is slightly higher, the resultant capacitance will not change too much unless the effect of roughness is significant. This did not seem to be the case. In all cases, an average line cross section was assumed through the middle of the rough ridges. In summary, the Table shows that the effect of roughness on effective DC resistivity and low-frequency effective dielectric constant are very small. This was also confirmed by measuring the characteristic impedance in TDR, Z_o. The impedance values for rough and smooth cards were within 1%.

Extraction of Total Loss

It was shown in [3], that a short-pulse propagation time-domain technique combined with signal processing and iterative fitting and modeling can successfully extract the total loss for representative stripline interconnects over the range 10 KHz to 50 GHz. It relies on a carefully built representative test vehicle that minimizes the interface discontinuities but retains all the key processing steps of an actual multi-layer card. High-bandwidth time-domain instrumentation and accessories are used such as the Agilent 86100B sampling oscilloscope with an 86118A, 70 GHz, detector unit connected through 65 GHz cables and coaxial probes (such as 67A from GGB Industries). In addition, the Picoseconds Pulse Labs 4022 TDT Source Pulse Enhancer and 5206 Differentiator allow the generation of 11 ps risetime step and 20 ps wide pulse excitations. Figs. 7a and b show an overall view of the measurement set-up and a close-up of the input and output coaxial probing. The 20-ps wide short pulse is launched on two identical lines of different lengths. Signal processing of the digitized, propagated pulses consists of rectangular time-windowing to eliminate reflections from pads, vias, probes, and the Fourier transformation into frequency-domain data. The two Fourier transforms are ratioed and from the ratio of the amplitudes and difference in phase, the attenuation, $\alpha(f)$, and phase constant, $\beta(f)$, are obtained. This is achieved without any calibration or de-embedding as used in network-analyzer based techniques. In the ratio operation, the effects of discontinuities will cancel out. Accurate sample cross sectioning is performed at many locations. Based on this, $R(f)$ and $L(f)$ per unit length can be calculated with a field solver such as CZ2D [4]. $C(f)$ and $G(f)$ can also be obtained with the same field solver if the complex permittivity is known. An initial starting set of values for the loss tangent at a few frequencies is given to the solver and the dielectric constant $\varepsilon_r^{'}$ at 1 MHz. The solver has a built-in Debye model for $\varepsilon(f)$ that guarantees causal response. Once the initial $R(f)$, $L(f)$, $C(f)$, and $G(f)$ are obtained, the calculated and measured attenuation and phase constant, $\alpha(f)$ and $\beta(f)$, are compared. A few iterations are made on the initial guess to improve the fit. The 1 MHz $\varepsilon_r^{'}$ is obtained from the capacitance measurement of the large circular plate placed on the signal layer. A few additional low frequency $\tan\delta$ values are added to the initial starting values. These are obtained from LCR-meter based $\tan\delta$ measurements of the plate in the 10 KHz to 1 MHz range. Having $C(f)$, $G(f)$, C_{1MHz}, and

$\varepsilon_{r\,1MHz}^{'}$ allows the broadband extraction of $\varepsilon_r^{'}(f)$ and tanδ*(f).* Fig. 8 shows a typical comparison of measured and calculated attenuation for the smooth card C. In this case the measurement bandwidth was 2.2 GHz to 38 GHz and the Debye model extrapolated the data over the 10 KHz to 50 GHz range. Fig. 9 shows the measured attenuations for all six card cases.

It has been proposed to use a Debye model to represent the slowly varying $\varepsilon_r^{'}(f)$ and tanδ*(f)* properties of most printed-circuit board insulator materials. It ensures causality for $\varepsilon(f)$ and is a good representation for the polarization-damping based losses. The analytic function below

$$\varepsilon(\omega) = \varepsilon_\infty + \sum_i \frac{\varepsilon_i}{1 + j\omega\tau_i} \tag{1}$$

can be calculated with a small number of poles. A typical representation for a good broadband model might have 30 poles over the range 10 KHz to 1000 GHz. Ten values could be specified and interpolation and piecewise linear expansion with respect to *log(f)* can be made to consistently determine both $\varepsilon_r^{'}(f)$ and tanδ*(f)* over the desired frequency range. Fig. 10 shows simulation results for a 38 cm long line and 6 Gbps transmission for four conditions. Simulation was made with ten initial tanδ values in the range of 10 GHz to 50 GHz, two values, namely at 1 MHz and 50 GHz, constant $\varepsilon_r^{'}$ and tanδ, and constant values without using a Debye model. It was found that the differences in amplitude were -28.3 mV, -8.5 mV, and +6.9 mV compared to the ten-value case with amplitude of 561 mV, respectively. The delay differences were -16 ps, -25 ps, and +70 ps , respectively. The accuracy of the model increases with the number of specified input values, however, all Debye-based models are much closer to each other and to measurements than when causality is not respected. For constant $\varepsilon_r^{'}$ and tanδ, $G = \omega C tan\delta$ expression is used with C at 1 MHz and this cannot provide consistency of complex $\varepsilon(f)$ and results in large simulation errors.

Effect of Surface Roughness

In order to eliminate the effect of slight differences in cross section, resistivity, and dielectric constants, a common cross section with a trapezoidal shape of width 91.9 / 109 μm (3.62 / 4.29 mil) or effective 100.5 μm (3.955 mil) and thickness of 32.0 μm (1.26 mil) was used for all three materials. The dielectric heights were $h_1 = h_2 = 114.0$ μm (4.49 mil). In all three cases, the conditions for *R(f), L(f), C(f),* and *G(f)* calculations were such that the fit was either made to the total loss for the smooth cards or the total loss for the roughened cards, but the cross section was the same. The $\varepsilon_{r\,1MHz}^{'}$ and ρ_{DC} that were used were extracted from measurements of the six actual cards of this study. Fig. 11 then shows the resultant six attenuations. The solid traces correspond to the smooth cards. The low-loss materials A and B have a substantial increase in total loss due to roughness. At 5 GHz, A and B cards have an increase in attenuation of 49.8% and 20.3%, respectively. At 10 GHz, the increase is 53.4% and 23.6%. Material A with roughened metallization produces a total interconnect loss that is very close to the loss of card C which is a standard material in use today. All the advantages of lower tanδ are overwhelmed by the losses due to roughness. Material C in fact has the least increase due to the ridges, namely at 5 GHz, only 5.5% increase, and at 10 GHz, 10.6%. It is possible that the newer materials require a more aggressive roughening process. Fig. 12 plots the differences in attenuation caused by roughness.

The values shown in Fig. 11 for the roughened cards were calculated by assuming an average cross section through the rough ridges. What this implies is that when extracting the effective $\varepsilon_r^{'}(f)$ and tanδ*(f),* the effect of roughness which is an additional resistive loss, gets attributed to dielectric loss. This is because the actual topography of the ridges is not accounted for. As a result, the error in the extracted tanδ is quite large as shown in Fig. 13. This issue has also been highlighted in [7] and attempts have been made to find analytical techniques fitted to measurements to alleviate this error. Fig. 14 shows the extracted dielectric constants for the smooth cards.

Modeling the Effect of Roughness

Including the actual profile of the ridges shown in Fig. 5 in any full-wave electromagnetic field solver can be extremely costly in the number of unknowns and run time. Attempts have been made to use stochastic techniques for the calculation of capacitance [8] and effective conductivity [9] but complete broadband causal model generation has not been attained. In this study, an attempt was made to continue using the two-dimensional field solver that was used for the smooth card analyses. An equivalent cross section is shown in Fig. 15 for card B. 7.5 μm tall rectangles with 8 μm and 5 μm widths and 3 μm separations represented the ridges. Each rectangle had a 1 μm shell of material with resistivity of ρ = 15 μΩcm. The ridges on the ground layer were represented by a thin, 5.5 μm, layer with ρ = 15 μΩcm. The extraction was then performed for *C(f)* and *G(f)* by using the tanδ values obtained for the smooth card. For the case of card C, the equivalent cross section had uniform ridges with widths of 10 μm, heights of 5.5 μm, and resistivity of 2.086 μΩcm. The ground ridges were represented by a 7.5 μm thick layer with resistivity of ρ = 50 μΩcm. This type of a simplification can only be achieved if both the smooth and roughened versions of the same build are available. This can, however, alleviate very costly computations and provide fairly

accurate, causal, predictive broadband models for system performance assessment. Notice that the 2D model will differ for each material and build condition. The attenuation differences are shown in Fig. 16 for card A and compared with measurements. For the rough case, results are compared for the cases where an average cross section through the middle of the ridges is assumed (no ridges), the case where only signal ridges are included in the modeling (signal ridges), and the case where both signal ridges and a high resistivity thin layer is included on the ground plane. The effect of the ridges on the ground plane is not large but it can add error in the prediction and should not be ignored. The magnitude of this error is shown in Fig. 16. Including all effects with this type of 2D modeling can provide a fairly good model over a wide frequency range and the model is guaranteed to be causal.

Simulations were also performed for two representative data-rates, namely 3 Gbps and 6 Gbps, with and without roughness-induced loss. 333 ps and 166 ps wide pulses were transmitted on 76.2 cm and 38 cm long lines, respectively, with the card B wiring and the common cross section described earlier for Fig. 11. For the 3 Gbps case, the loss in useable length was 2.12 cm (2.8%), the loss in amplitude was 1.8%, and the delay increase was 95.6 ps or 1.9%. In the case of 6 Gbps, as shown in Fig. 17, the loss in useable length was 4 cm or 10.5%, the increase in delay was 44 ps or 1.8%, and the decrease in signal amplitude was 17.5%.

Conclusions

It has been shown that resistive losses caused by the roughening of metallization in printed-circuit board wiring can be quite significant. The increase of total loss ranged from 5.5% to 49.5%, even at 5 GHz. The use of roughness to promote adhesion can cancel the beneficial low dielectric loss characteristics of newly developed card insulators and manufacturers need to thrive to eliminate the rough ridges. The effect on signal integrity was shown to increase with frequency and could curtail the delivery of high-performance systems or increase system complexity and cost.

One of the most significant finding of the study was that this effect will be quite different in characteristic depending on material used by card manufacturer and treatment employed by supplier of metal foil. The rough ridge profile could even differ on the ground plane layer from the signal line layer within the same card cross section. The coating of the lines and the composition of the micro-nodules is not generally released or known by vendors and the effective resistivity can be significantly higher than for copper metallization. The resultant composite cross section cannot be predicted. Moreover, accurate three-dimensional modeling is prohibitive in computation cost. Even faster stochastic modeling approaches require cross sectional information which is hard to obtain. This is then the second significant finding of the paper, namely that any modeling technique requires some amount of fitting to actual hardware. Because of this, a practical approach that circumvents costly analyses was outlined in this paper. It relies on the availability of a smooth version of the card build for each material considered. This allows the use of fast, two-dimensional modeling techniques for generating causal, broadband, predictive models for simulation. The implicit assumption is that the two card constructions maintain the same insulator properties. Card manufacturers are hard at work in developing new processing techniques that can use profile-free copper as was recently shown in [10] and one such cross section is shown in Fig. 18. The smooth material can result in lower total attenuation than the combination of low tanδ and roughened foil. This might relax the material development requirements and afford higher data rate transmission. Reliability testing on large multi-layer boards is still underway for these newer options.

References

[1] A. E. Ruehli and A. C. Cangellaris, “Methodology for the electrical modeling of interconnects and electronic packages”, Proc. IEEE, vol. 89, no. 5, pp. 740-771, May 2001.

[2] K. M. Cooperich, J. Morsey, A. C. Cangellaris, and A. E. Ruehli, “Physically consistent transmission line models for high-speed interconnects in lossy dielectrics”, in Proc. IEEE 10th Topical Meeting on Electrical Performance of Electronic Packaging, EPEP, Cambridge, MA, Oct. 29-31, 2001, pp. 247-250.

[3] A. Deutsch, T-M. Winkel, G. V. Kopcsay, C. W. Surovic, B. J. Rubin, G. A. Katopis, B. J. Chamberlin, R. S. Krabbenhoft, “Extraction of $\varepsilon(f)$ and $\tan\delta(f)$ for Printed-Circuit Board Insulators up to 30 GHz Using the Short-Pulse Propagation Technique”, IEEE Trans. On Adv. Packg., vol. 28, no. 1, pp.4-9, Feb. 2005.

[4] W. T. Weeks, L. L. Wu, M. F. McAllister, and A. Singh, “Resistive and inductive skin effect in rectangular conductors”, IBM. J. Res. And Dev., vol. 23, pp.652-660, 1979.

[5] http://www.gould.com/cf_jtc.htm

[6] B. L. Adams-Melvin, D. R. McGregor, K. H. Dietz, “eefects of Copper Foil Type and Surface Preparation on Fine Line Image Transfer in Primary Imaging of Printed Wiring Boards”, digest PC World Convention VII, pp. 1-20, Basel, Switzerland, May 21-24, 1996.

[7] G. Brist, S. Hall, S. Clouser, T. Liang, “Non-Classical Conductor Losses Due to Copper Foil Roughness and Treatment”, digest ECWC10 Conference at APEX IPC Printed Circuits Expo and Designers Summit 2005, pp. 1-11, Feb. 22-24, 2005, Anaheim, CA.

[8] Z. Zhu, “Efficient Integral Equation Based Algorithms for Parasitic extraction of Interconnects with Smooth or Rough Surfaces”, PhD Thesis MIT, Aug. 2004. http://www.rle.mit.edu/cpg/people-alumni.htm.

[9] L. Proekt and A. C. Cangellaris, “Investigation of the Impact of Conductor Surface Roughness on Interconnect Frequency-Dependent Ohmic Loss”, 2003 ECTC Conference, pp.1004-1010, June 2003, New Orleans, LA.

[10] N. Ogawa, H. Onezeki, N. Moriike, T. Tanabe, T. Kumakura, “Profile-Free Copper Foil for High-Density Packaging Substrates and High-Frequency Applications”, Proc. 2005 Electronic Components and Technology Conference, Las Vegas, NV, pp.457-461.

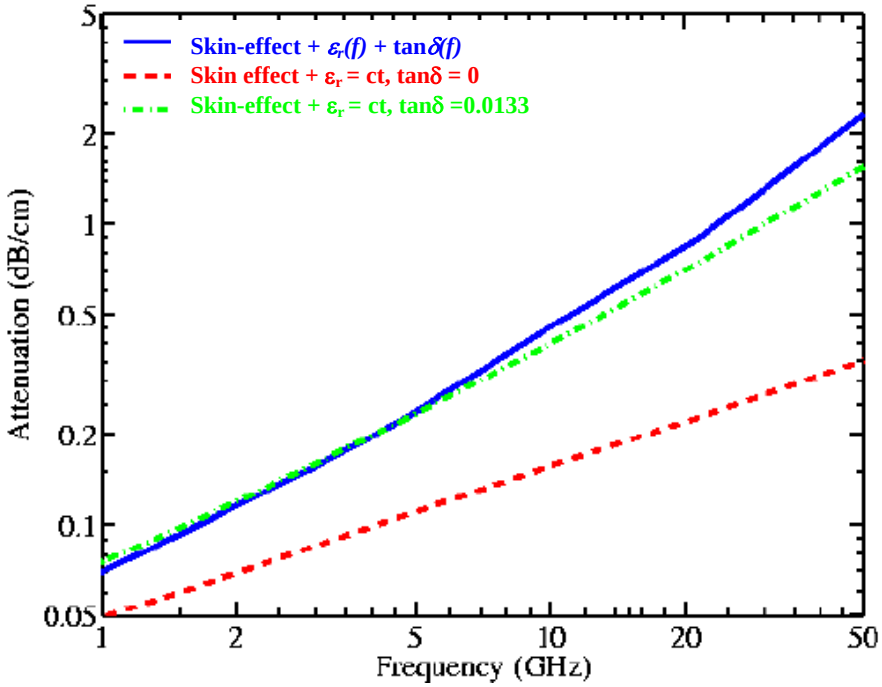

Fig. 1 Calculated attenuations for complex permittivity $\varepsilon(f)$ (solid), constant ε_r and $\tan\delta=0$ (dashed), and constant ε_r and $\tan\delta = 0.0133$ (dot-dashed) for card B.

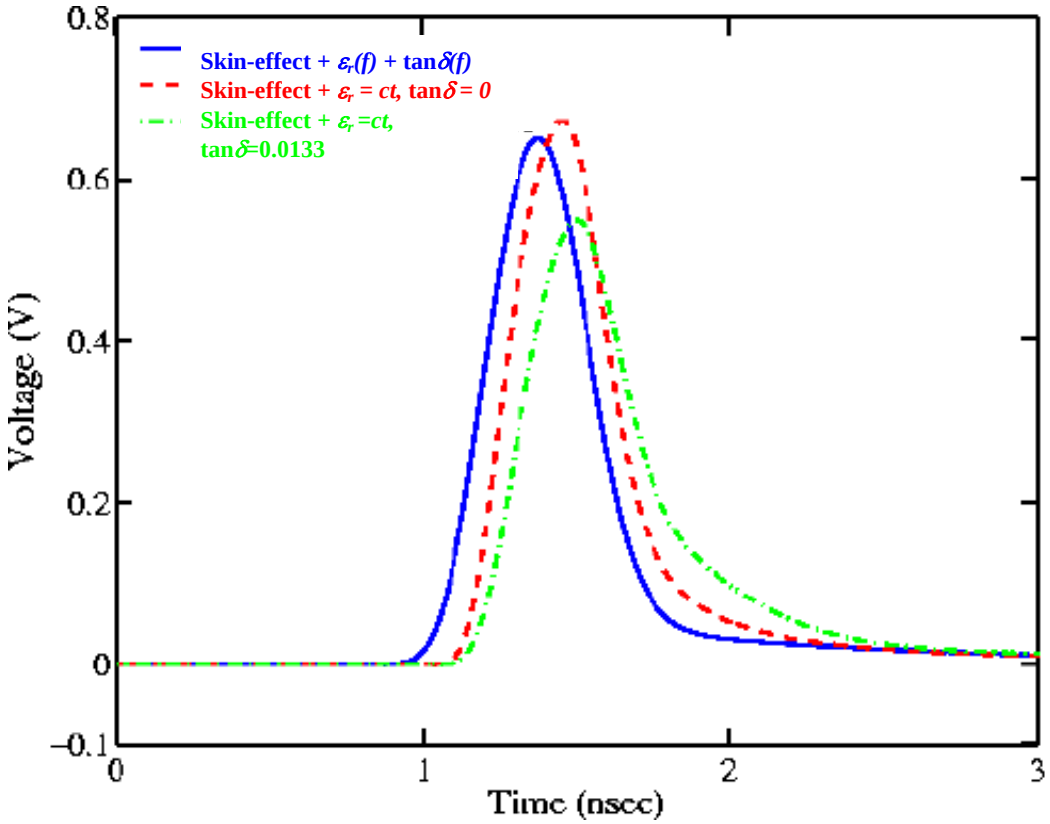

Fig. 2 Simulated 333-ps wide pulses (3 Gbps) propagated on 4x1.26 mil cross section lines for the three cases of Fig. 1.

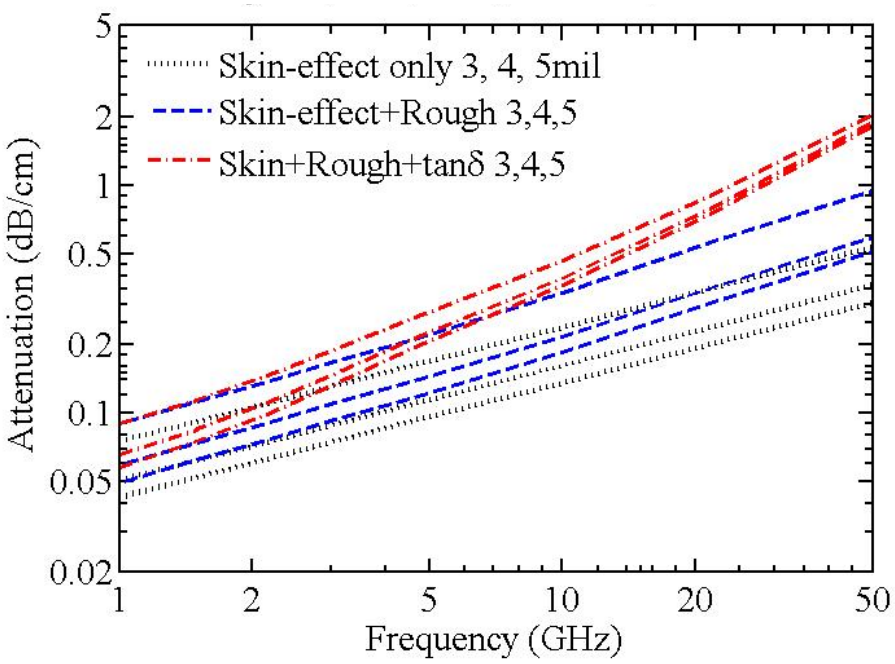

Fig. 3 Calculated attenuation for 3.0 mil 0.5 oz, 4 mil 1 oz, and 5 mil, 1 oz lines with card B material for cases of skin-effect only (dotted), skin-effect and roughness induced resistive losses (dashed), and all losses including dielectric loss (dot-dashed).

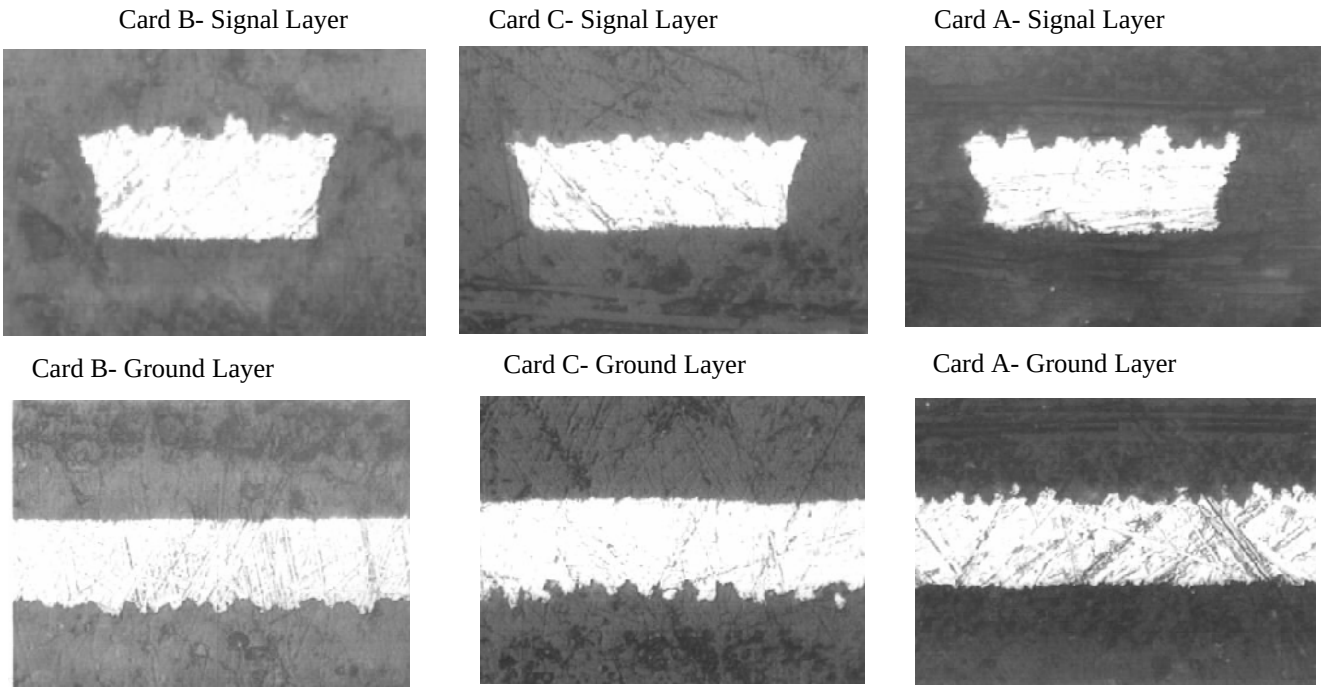

Fig. 4 Typical signal and ground-plane cross sections for cards A, B, and C with rough metallization. The bottom views show the ground planes for each case.

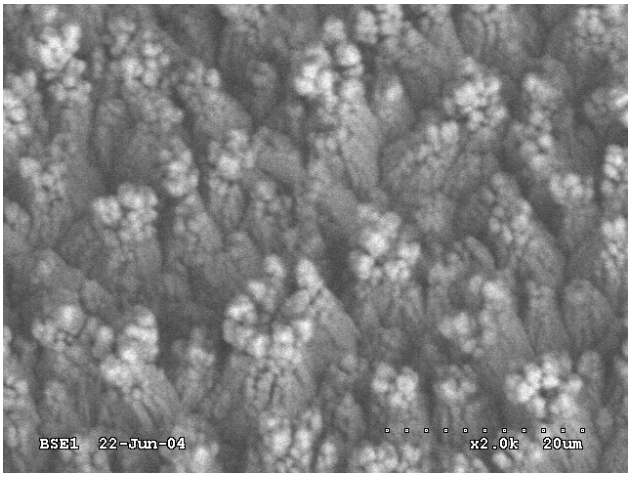

Fig. 5 Top view of typical rough ridges.

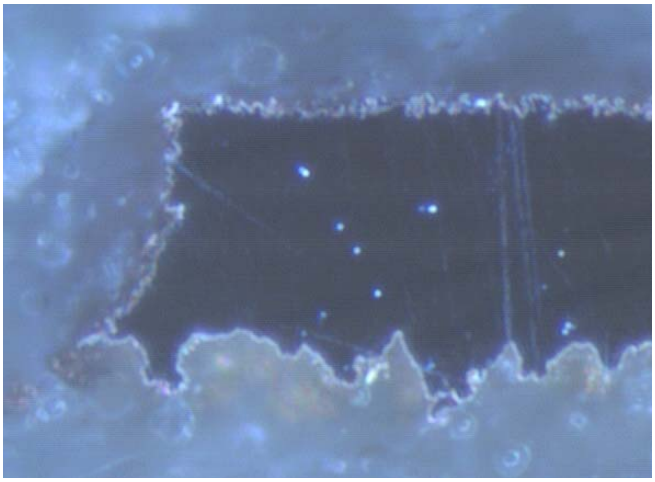

Fig. 6 Close up of thin coating of the rough ridges.

a)

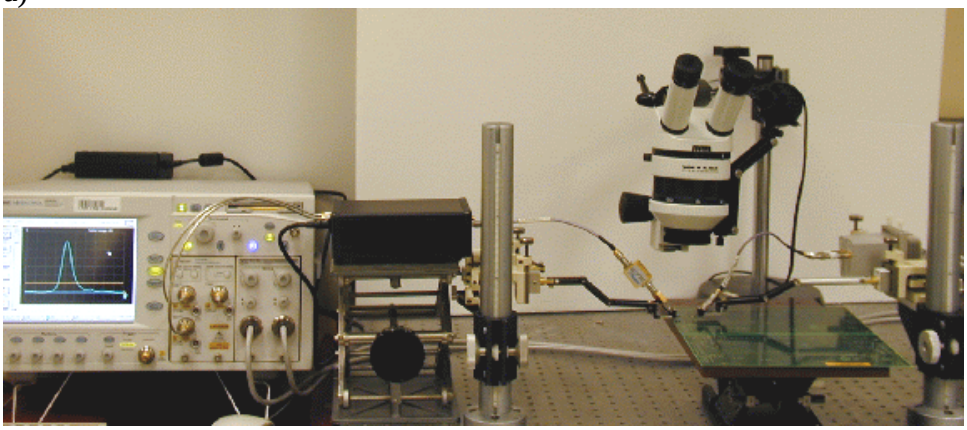

b)

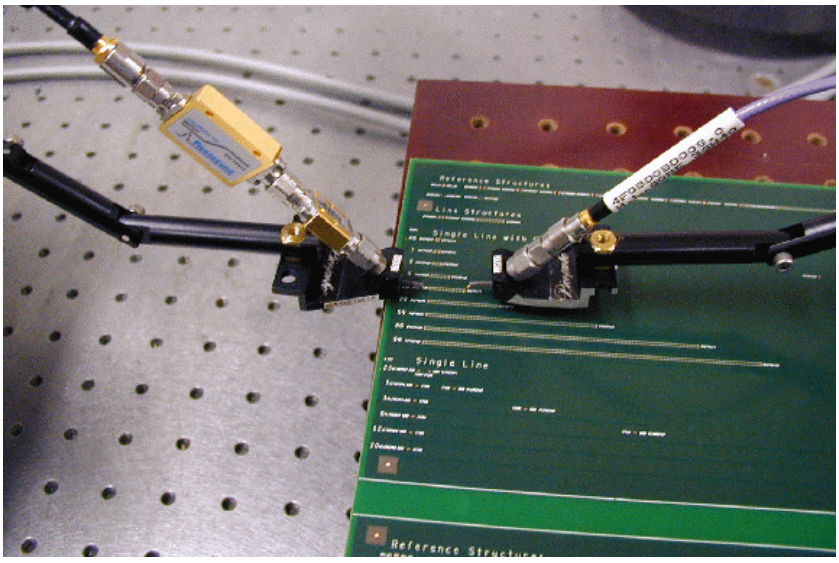

Fig. 7 a) Overview of test system set-up with 70 GHz detector, b) and close-up view of the input and output probes, the input pulse enhancer module, and the passive differentiator.

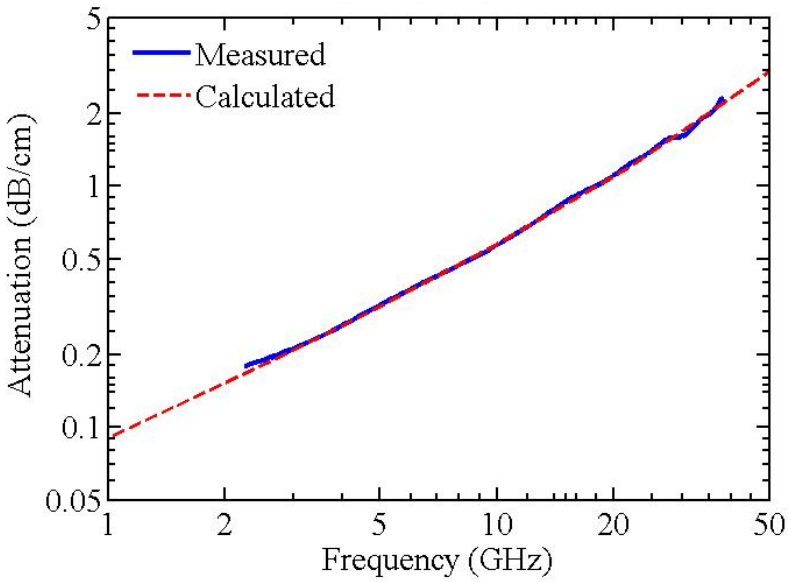

Fig. 8 Measured and calculated $\alpha(f)$ for smooth card C.

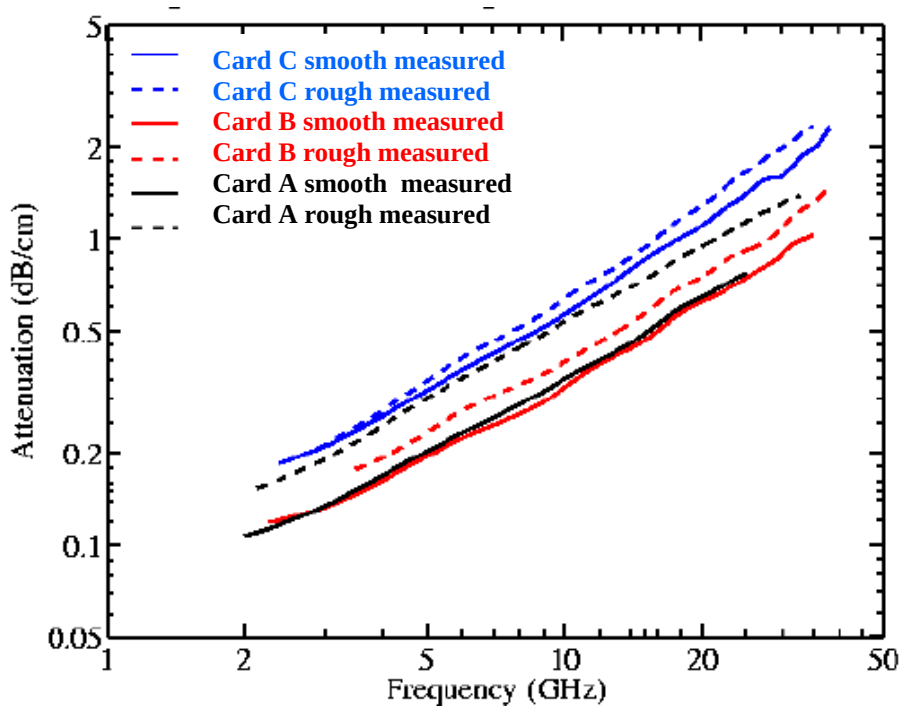

Fig. 9 Measured attenuations for the six cards with rough and smooth metallization.

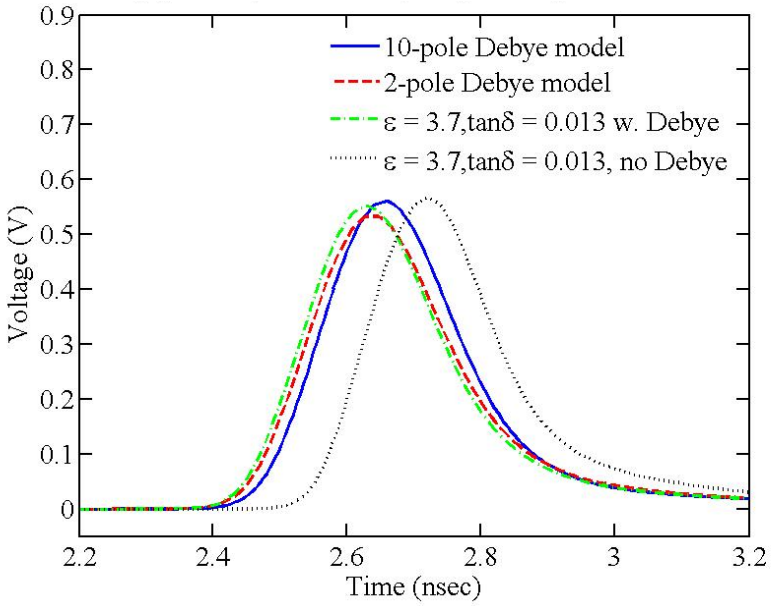

Fig. 10 . Simulated 6 Gbps response for 38 cm trace on card B.

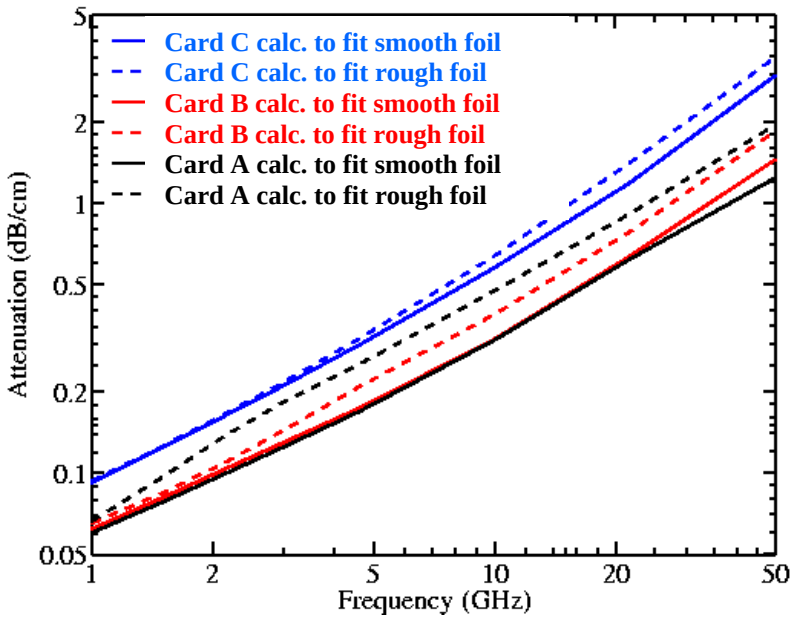

Fig. 11 Calculated attenuations for the three smooth (solid) and three roughened cards (dashed) with the common cross section.

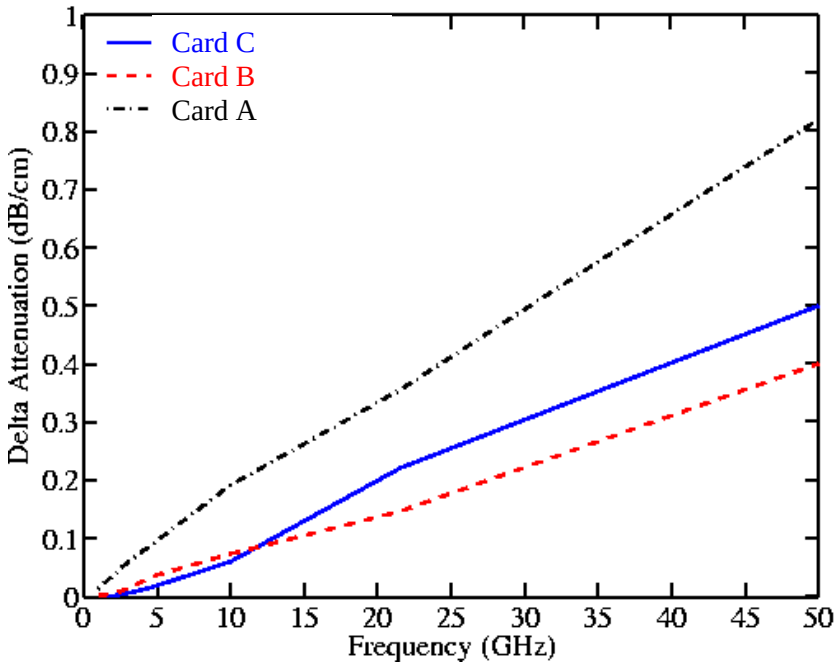

Fig. 12 The difference in attenuation between rough and smooth cards for the cases shown in Fig. 11.

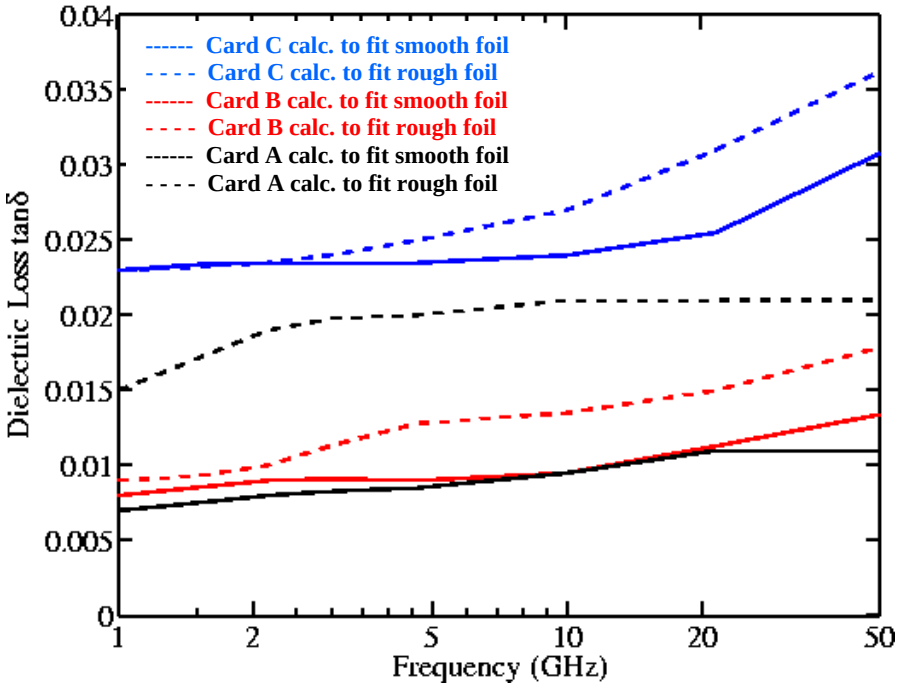

Fig. 13 Extracted dielectric loss for the six cases in Fig. 9.

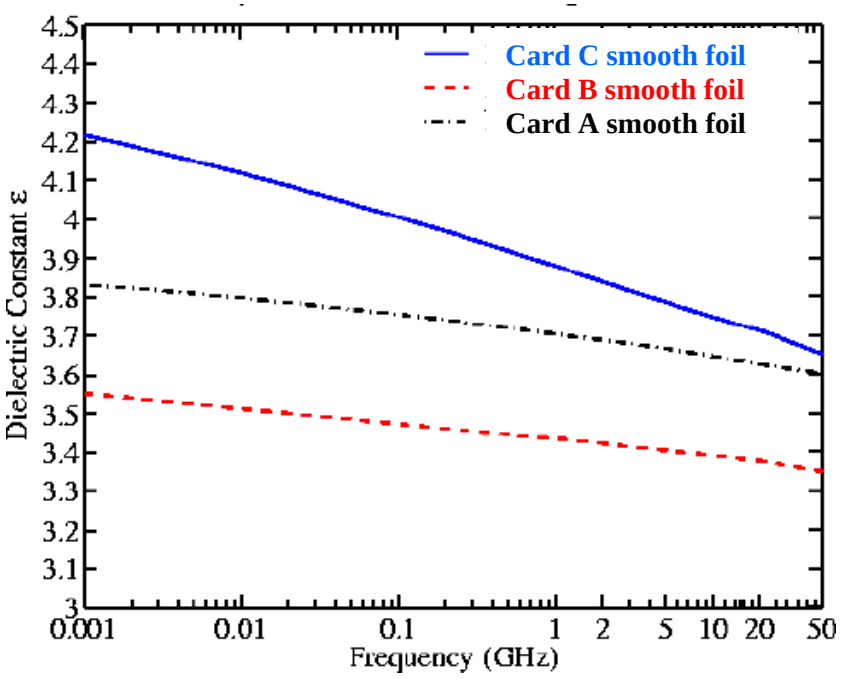

Fig. 14 Extracted dielectric constant for the smooth cards of Fig. 9.

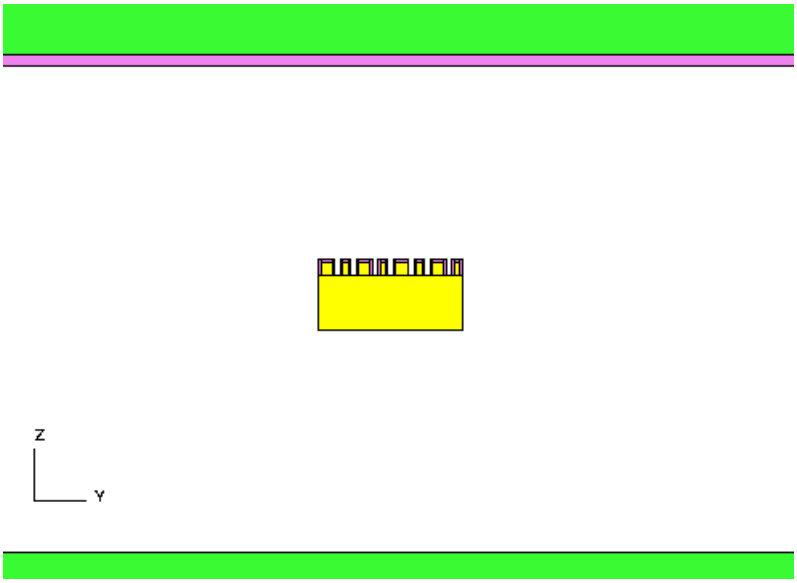

Fig. 15 Two-dimensional model used for roughened card B.

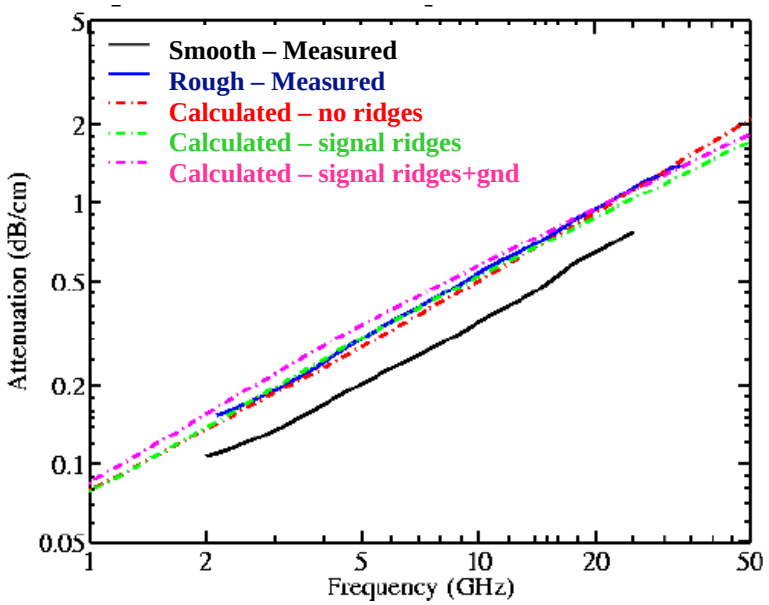

Fig. 16 Measured and calculated attenuations using the model shown in Fig. 15.

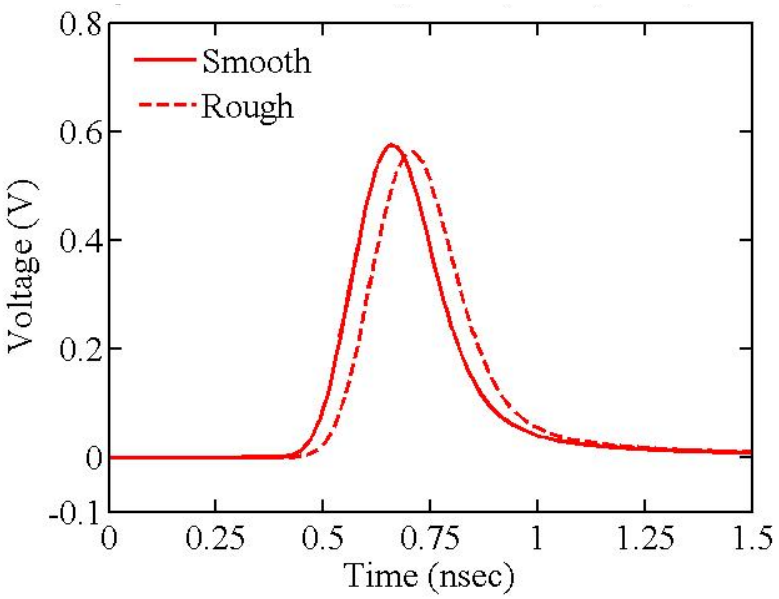

Fig. 17 Simulated 6 Gbps response for 38-cm long trace on card B with smooth (solid) and roughened (dashed) metallization.

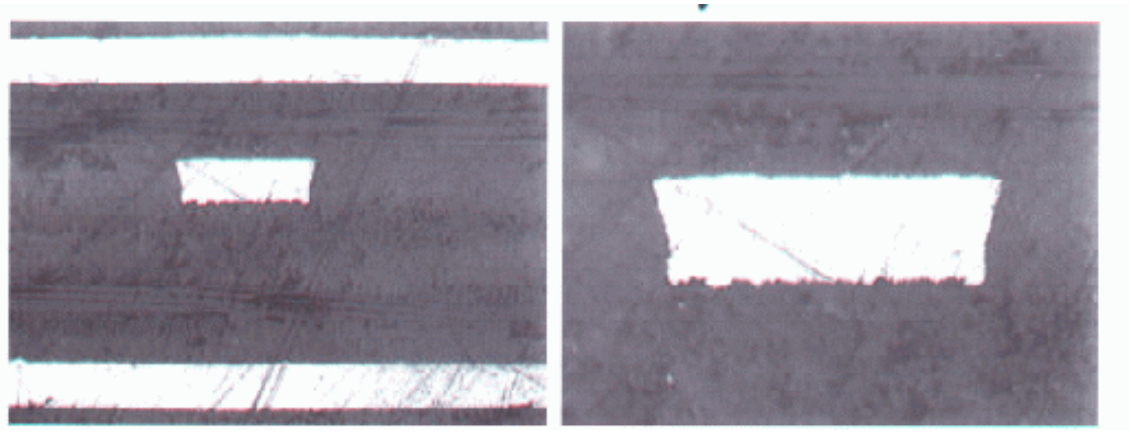

Fig. 18 Cross section of newer material with extremely small roughening.

TABLE

Smooth	Rough	
Card A ρ = 2.096 $\mu\Omega$cm,	ρ = 2.097 $\mu\Omega$cm	Δ = 0.05%
Card B ρ = 2.070 $\mu\Omega$cm,	ρ = 2.080 $\mu\Omega$cm	Δ = 0.50%
Card C ρ = 2.073 $\mu\Omega$cm,	ρ = 2.086 $\mu\Omega$cm	Δ = 0.60%
Card A ε_r = 3.45	ε_r = 3.60	Δ = 4.3%
Card B ε_r = 3.55	ε_r = 3.70	Δ = 4.2%
Card C ε_r = 4.10	ε_r = 4.20	Δ = 2.4%
Card A R = 0.069 Ω/cm	R = 0.0725 Ω/cm	Δ = 5.07%
Card B R = 0.080 Ω/cm	R = 0.0880 Ω/cm	Δ = 10.0%
Card C R = 0.065 Ω/cm	R = 0.0670 Ω/cm	Δ = 3.00%
Card A Area = 3038mm^2	Area = 2893mm^2	Δ = -4.8%
Card B Area = 2592mm^2	Area = 2368mm^2	Δ = -8.6%
Card C Area = 3184mm^2	Area = 3123mm^2	Δ = -1.9%
Card A C_{mes} = 1.366 pF/cm	C_{mes} = 1.408 pF/cm	Δ = 3.1%
Card B C_{mes} = 1.200 pF/cm	C_{mes} = 1.215 pF/cm	Δ = 1.3%
Card C C_{mes} = 1.440 pF/cm	C_{mes} = 1.473 pF/cm	Δ = 2.3%
Card A h = 106/95 μm	h = 103/97 μm	
Card B h = 103/115 μm	h = 103/114 μm	
Card C h = 103/137 μm	h = 111/133 μm	